Journal of Cardiovascular Disease Research

ISSN: 0975-3583,0976-2833 VOL14, ISSUE 07, 2023

Screening and discovery of novel carbamate compounds for cancer therapy

Dr. Lavanya Yaidikar[1], Pydiraju Kondrapu[2], Astha Mishra[3], Pramod Bhaskar Kumar[4], Dr. Arshad Ahmad[5], Dr. Shaima K A[6], Dr. Chamaraja N A[7], Dr. Shubhangi Tripathi[8]*

[1] Professor, Seven Hills College of Pharmacy, Tirupati-517561, Andhra Pradesh
[2] Assistant Professor, Aditya pharmacy college, Surampalem, ADB road, kakinada district, A.P. 533437
[3] Assistant Professor, Sagar institute of technology and management department of pharmacy
[4] Associate Professor, Shree Devi College of Pharmacy. (RGUHS. Karnataka). Airport road.Kenjar.Mangalore.DK 574142.Karnatakae
[5] Professor, NGI College of Pharmacy, Modipuram Meerut UP- 250110
[6] Associate Professor, Shambhunath Institute of Pharmacy, Jhalwa, Prayagraj, Uttar Pradesh 211012
[7] Assistant Professor, Department of Chemistry, JSS Academy of Technical Education (Affiliated to Visvesvaraya Technological University, Belagavi), Dr.Vishnuvardhan Road, Bengaluru 560 060, India
[8] Assistant Professor, J. N. L. College, Khagaul, Patna 801105, Patliputra University, Patna

***Corresponding Author Details:Dr. Shubhangi Tripathi**

drshubhangitripathi@gmail.com

ABSTRACT

A 33 KDa serine hydrolase enzyme known as monoacylglycerol lipase is associated with a number of physiological processes in people, including pain, inflammation, and neurodegenerative diseases. The enzyme has been discovered to be associated with the endocannabinoid lipid signalling network system and has been found to be present in both the central and peripheral nervous systems. Enzyme support the growth of cancer and tumour cells by acting as a source of free fatty acids. It has been noted that the enzyme's activity is elevated in dividing and expanding cells in a number of cancer types. The signalling molecules phosphotidic acid, lysophosphatidic acid, sphingosine phosphate, and prostaglandin E2 are found to be free fatty acid-derived and have been linked to the proliferation, migration, and survival of cancer cells. They also rise as a result of enzyme activity. In the current work, we have carried out the identification task and screening investigation for the newly developed carbamate derivatives as anti-cancer moieties using docking and other computational tools.

Keywords: Enzyme, Inhibitors, Monoacylglycerol, Lipase, Cancer, Inflammation.

Introduction

The Monoacylglycerol Lipase (MAGL), a membrane-bound serine hydrolase (Castelli et al., 2020; Jiang & Van Der Stelt, 2018; Malamas et al., 2020; L. Zhang et al., 2019) prevalent in peripheral organs such as the liver, kidney, testis, lungs, prostate, and small intestine as well as the central nervous system, is crucial to the endocannabinoid system (Dato et al., 2020). The endocannabinoid system (eCB) is a lipid signalling network that has been discovered to be present in both the central and peripheral nervous systems (Z. Chen, Mori, Fu, et al., 2019;

ISSN: 0975-3583,0976-2833 VOL14, ISSUE 07, 2023

Kind & Kursula, 2019; Mori et al., 2019). It is known to play a significant role in the regulation of a

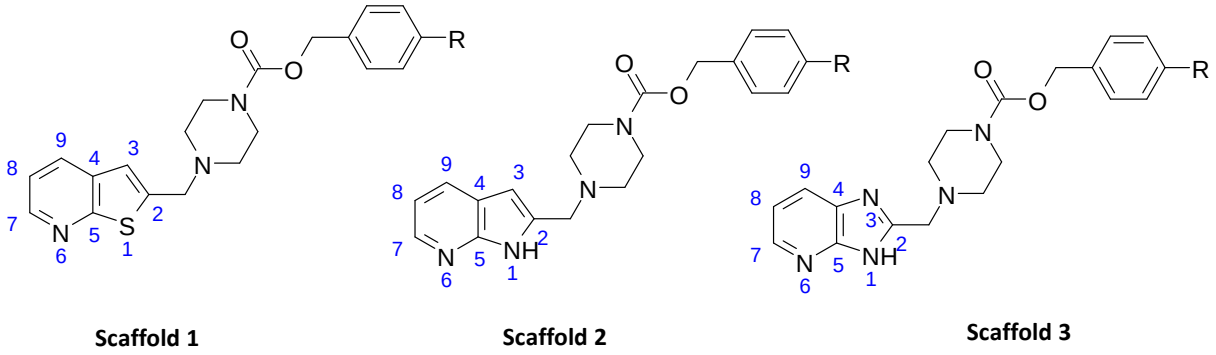

Fig. 1 Scaffolds of newly designed carbamate derivatives

Table 1. List of different designed derivatives of Scaffold 1, scaffold 2, scaffold 3 and their docking score.

S. No.	R = Substitution	Ligand Code	Binding Energy	Ligand Code	Binding Energy	Ligand Code	Binding Energy
1.	H	TH101	-10.5	TH201	-10.8	TH301	-10.6
2.	NO2	TH102	-10.9	TH202	-11.2	TH302	-10.8
3.	Cl	TH103	-11.1	TH203	-11.2	TH303	-10.9
4.	Br	TH104	-11.1	TH204	-11.2	TH304	-11
5.	F	TH105	-11.1	TH205	-11.4	TH305	-10.9
6.	CH3	TH106	-11.1	TH206	-11.5	TH306	-11.1
7.	CH2CH3	TH107	-10.8	TH207	-11.4	TH307	-10.4
8.	CH2CH2CH3	TH108	-11.5	TH208	-11.5	TH308	-11.1
9.	CH2CH2CH2CH3	TH109	-11.4	TH209	-11.4	TH309	-11
1(	NH2	TH110	-10.4	TH210	-11.1	TH310	-10.3
11	NHCH3	TH111	-10.5	TH211	-9.7	TH311	-9.7
12	NHCH2CH3	TH112	-10	TH212	-10.2	TH312	-9.8
13	NHCH2CH2CH3	TH113	-10.1	TH213	-11.3	TH313	-9.9
14	OH	TH114	-10.7	TH214	-11.1	TH314	-10.7
15	OCH3	TH115	-10.4	TH215	-11.1	TH315	-9.9
16	OCH2CH3	TH116	-10.6	TH216	-11	TH316	-9.7
17	OCH2CH2CH3	TH117	-11.3	TH217	-11.2	TH317	-10

number of processes, including appetite (Miceli et al., 2019), stress response, cognition, immune response, neurotransmission, learning, sleep regulation, reproduction, and pain perception (Z. Chen, Mori, Deng, et al., 2019; Hattori et al., 2019; Kind & Kursula, 2019). Two membrane-bound G protein-coupled receptors, CB1 and CB2, make up the endocannabinoid system. These receptors contain the endocannabinoids N-arachidonoyl ethanolamine (anandamide; AEA) and 2-arachidonoylglycerol (2-AG) (Z. Chen, Mori, Deng, et al., 2019; Granchi et al., 2019; Hattori et al., 2019). The / hydrolase superfamily includes MAGL and FAAH also (Kohnz & Nomura, 2014; Scalvini, Vacondio, et al., 2016b). Fatty acid hydrolase (FAAH), is found to hydrolyze anandamide (Kohnz & Nomura, 2014; Liu et al., 2016),

ISSN: 0975-3583,0976-2833 VOL14, ISSUE 07, 2023

whereas monoacylglycerol lipase (MAGL) hydrolyzes 2-AG primarily (Granchi et al., 2018, 2019), up to 85% (Granchi et al., 2019), with a minor

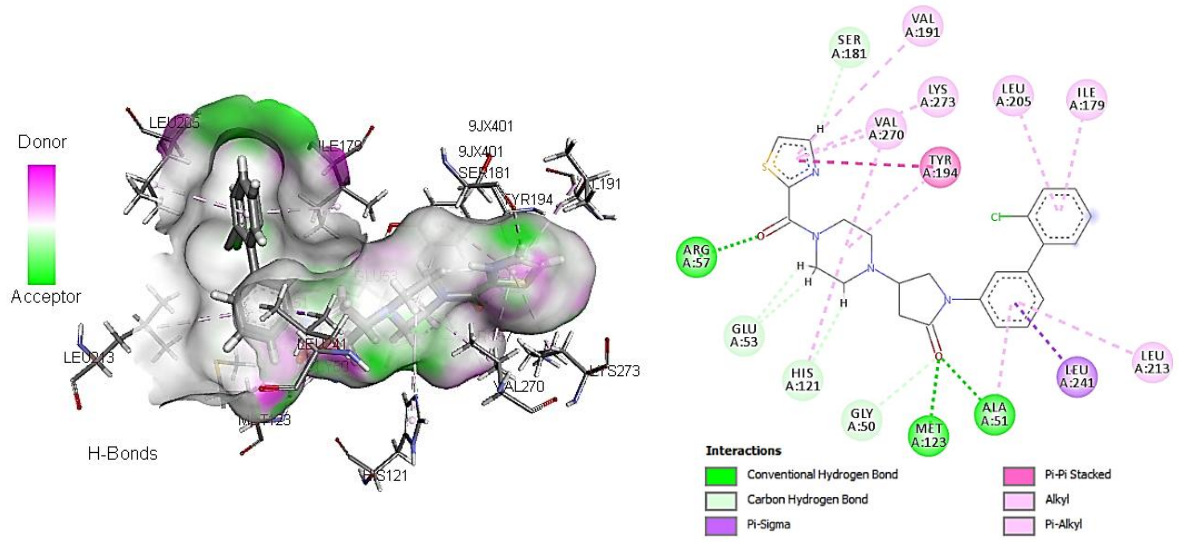

Fig. 2. Redocking pose of ligand 9JX with protein 5JN and binding interaction of Ligand 9JX with different residues in protein 5ZUN.

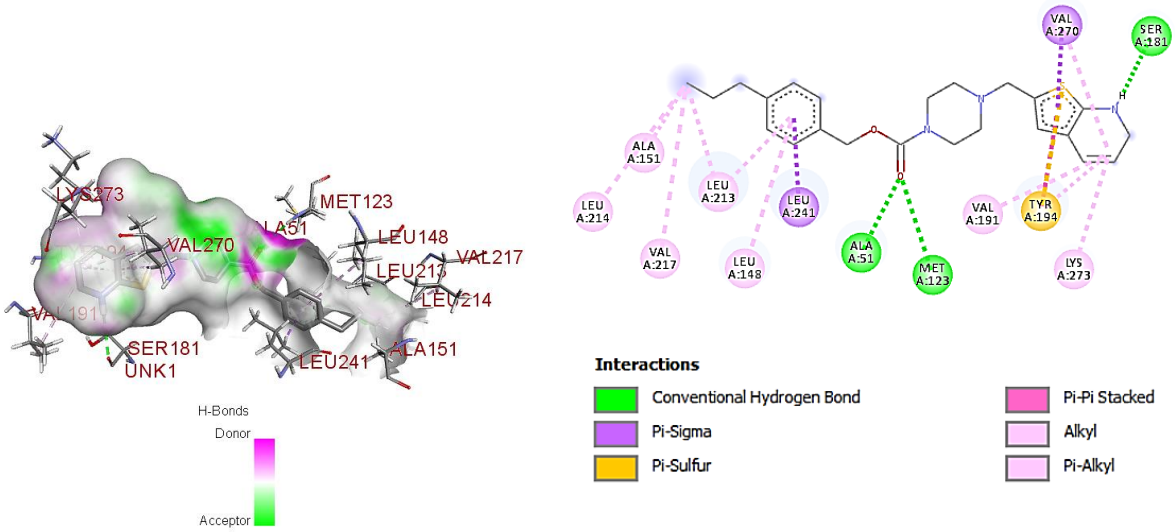

Fig. 3. 3D and 2D Docking images of ligand FH108 of series 01.

participation from / hydrolase-6 and -12 (ABHD6 and ABHD12) (Patel et al., 2015; Scalvini, Piomelli, et al., 2016; Wang et al., 2016), releasing the pro-inflammatory eicosanoid precursor arachidonic acid (AA) and glycerol (Aida et al., 2018; Cisar et al., 2018; Granchi et al., 2018), While cytosolic phospholipase A2 hydrolyzes

ISSN: 0975-3583,0976-2833 VOL14, ISSUE 07, 2023

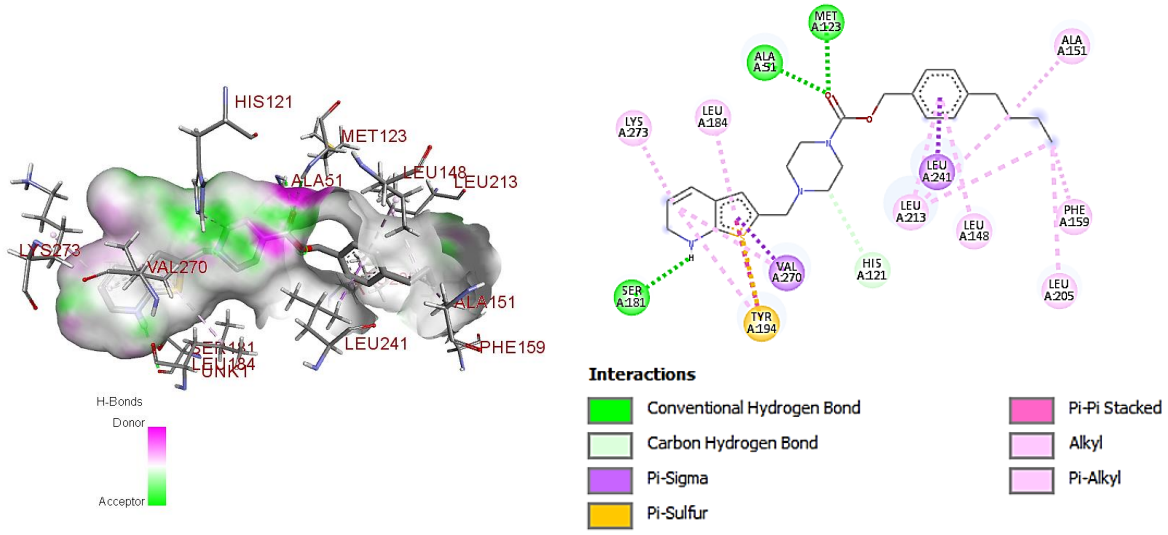

Fig. 4. 3D and 2D Docking images of ligand FH109 of series 01.

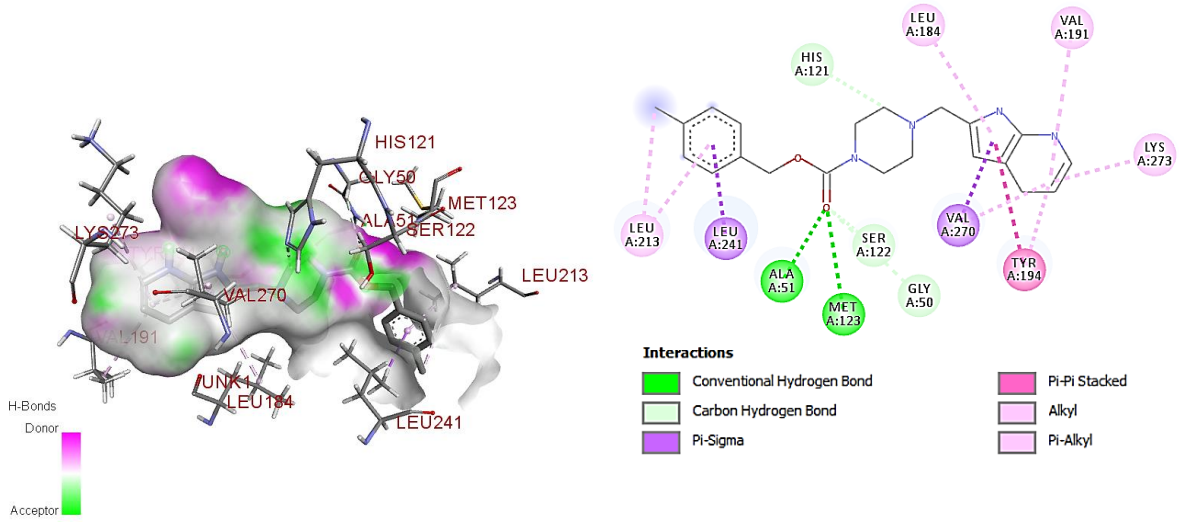

Fig. 5. 3D and 2D Docking images of ligand FH206 of Series 02.

phospholipids to form AA in the peripheral tissues (Butler et al., 2017), 2-AG hydrolysis through the MAGL, accounts for 50% production of AA in the brain (Mori et al., 2019) Therefore, suppression of the MAGL can result in a rise in 2-AG levels, which activates the cannabinoid neurotransmission system and causes the brain to experience antinociceptive (Wang et al., 2016), anti-anxiety, anti - emetic, anti-inflammatory, and neuroprotective effects (Ahamed et al., 2017a; Wang et al., 2016). In the brain, 2-AG serves as a significant source of arachidonic acid(Jiang & Van Der Stelt, 2018) and a precursor to prostaglandins that promote inflammation (Jiang & Van Der Stelt, 2018; L. Zhang et al., 2019) through its effects on CB1 and CB2

ISSN: 0975-3583,0976-2833 VOL14, ISSUE 07, 2023

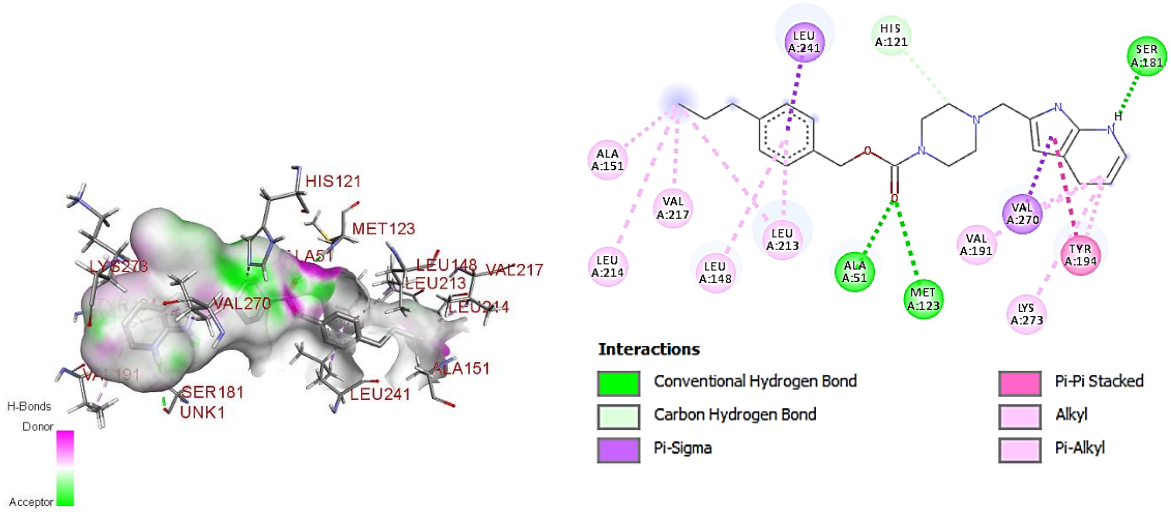

Fig. 6. 3D and 2D Docking Images of ligand TH208 of series 02.

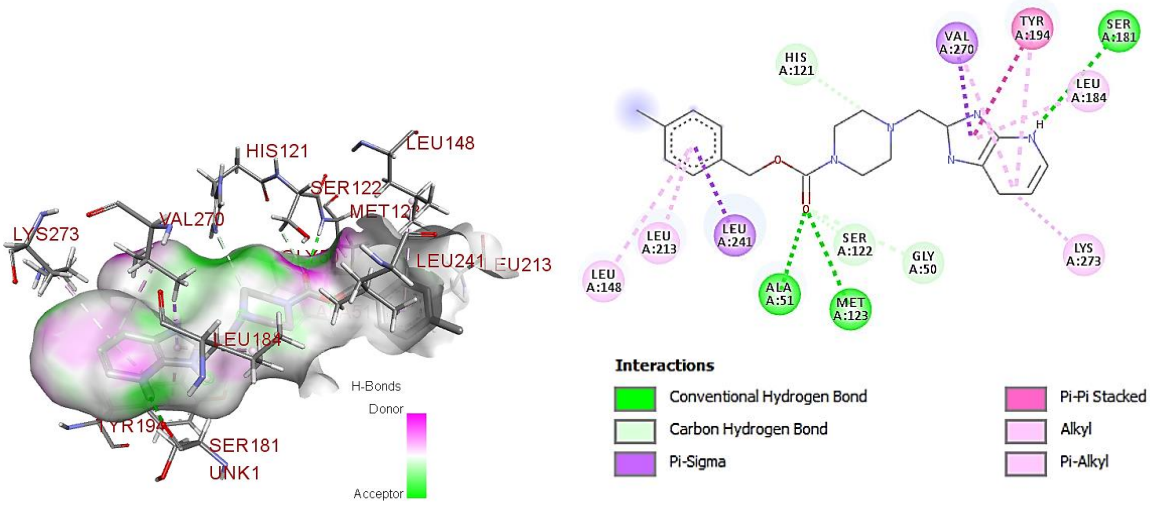

Fig. 7. 3D and 2D Docking images of ligand TH306 of series 03.

receptors, 2-AG can demonstrate its therapeutic effects on neuroinflammation (Ahamed et al., 2017a) and neuroinflammation is found to be common cause of neurodegenerative disorders (Kumar Verma et al., 2021; Verma et al., 2021). An increase in 2-AG signalling and a decrease in AA levels are brought about by MAGL inhibition, which has anti-inflammatory and gastrointestinal protective effects (Ahamed et al., 2017b; Riccardi et al., 2017).

Additionally, lipogenesis was discovered to be a factor in the proliferation of cancer cells. The lipolytic pathway, which releases the stored fatty acids for metabolic and signalling mechanisms, is also present in cancer cells. MAGL levels have been found

ISSN: 0975-3583,0976-2833 VOL14, ISSUE 07, 2023

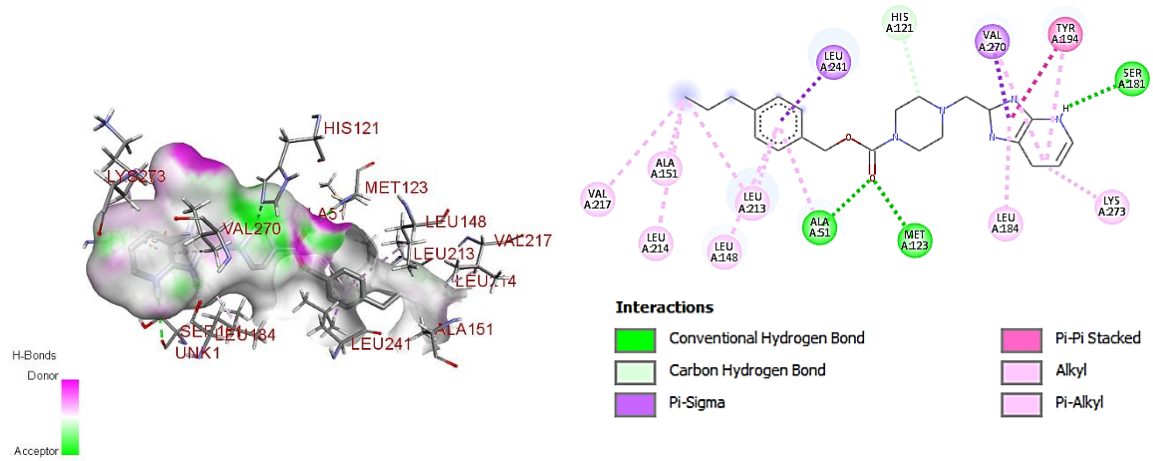

Fig. 8. 3D and 2D Docking Images of ligand 308 of series 03.

Table 2. Top three ligands Docking Scores of series 01, series 02 and series 03.

S. No.	Ligand	Binding Energy
1.	9JX	-13.4
2.	TH108	-11.5
3.	TH109	-11.4
4.	TH117	-11.3
5.	TH206	-11.5
6.	TH208	-11.5
7.	TH205	-11.4
8.	TH306	-11.1
9.	TH308	-11.1
10.	TH304	-11

to be much higher in aggressive cancer cells than in non-aggressive cancer cells (Granchi et al., 2018). Moreover, the high MAGL action is reported in aggressive cancer cells with their high serine hydrolase activity (Bononi et al., 2018a). Monoacylglycerol hydrolysis by MAGL regulates the levels of free fatty acids in healthy cells. It has also been discovered that MAGL is involved in the regulation of FFA levels in cancer cells (Ma et al., 2016). The MAGL-FFA pathway stimulates tumour growth, by providing feed into a complex lipid network enriched in pro-tumorigenic signalling molecules (Afzal et al., 2016; J. Zhang et al., 2016). The specific FFA-derived signalling lipids that are carcinogenic in nature, such as phosphatidic acid (PA), lysophosphatidic acid (LPA), sphingosine-1-phosphate (S1P), and prostaglandin E2, are likewise increased by MAGL activation (PGE2) (Afzal et al., 2016; Ahamed et al., 2017b). MAGL utilises a nucleophile-histidine-aspartate
catalytic triad in conjunction with an oxyanion hole for catalysis and is a member of the /-Hydrolase superfamily (Scalvini, Vacondio, et al., 2016a). With 303 amino acid residues, MAGL is a 33 kDa enzyme (Bononi et al., 2018b; Hattori et al., 2019). The cytosolic hydrolase MAGL is found responsible for breaking down monoacylglycerol (2-AG) into glycerol and free fatty acids (Afzal et al., 2014; Bononi et al., 2018b). The human MAGL shares the alpha/beta hydrolase fold (Jung & Piomelli, 2016; Karageorgos et al., 2017; Riccardi et al., 2017; Scalvini, Vacondio, et al., 2016b) with 8 beta-sheets, forming a partial beta-barrel that is

ISSN: 0975-3583,0976-2833 VOL14, ISSUE 07, 2023

embellished on both sides with 8 alpha-helices (King et al., 2009; Wise et al., 2012). The catalytic triad of a serine, carboxylic acid, histidine and other amino acids makes up the protein's active site, which is located between the alpha and beta helices (Afzal et al., 2014; Riccardi et al., 2017; Scalvini, Piomelli, et al., 2016). The long aliphatic chain of the natural substrate 2-AG is accommodated by the vast hydrophobic tunnel that forms the acyl chain binding area (ACB pocket) at the substrate's binding site. Ser122, His269, and Asp239 are the three amino acids that make up the catalytic triad at the head part of the ACB pocket (Bononi et al., 2018b; McAllister et al., 2018; Riccardi et al., 2017). The Ser122 is activated by the catalytic triad site and leads a nucleophilic attack on the carbonyl carbon of 2-AG. The connecting loop α1 and β3 (Gly50, Ala51, Met123, and Gly124) and the conserved network of hydrogen donors is known as the oxyanion hole (Afzal et al., 2014). The generated negative charge on the carbonyl in the transition state is stabilised by the presence of two backbone amide residues in the oxyanion hole in this region. A cytoplasmic access channel (CA channel), which contains additional polar residue, exists in addition to the catalytic triad. The hydrophilic glycerol moiety of 2-AG interacts with these polar residues of the channel, and upon hydrolysis, the glycerol moiety is released. Additionally, a considerable portion of the MAGL binding pocket is amphiphilic and hydrophobic, necessitating significant lipophilicity for both binding and inhibition. It is also known as the lipophilic portion of the ACB pocket (McAllister et al., 2018).

In the present work, we have carried out the identification and screening study for the newly designed carbamate derivatives as anti-cancer moieties utilising docking and other computational tools. (Perpetua-10)

Materials and Methods

1. Docking Studies Performed

Hardware and software used in study:

The HP laptop 64-bit outfitted with Windows 11 operating system, single language, Intel(R) Core TM i3-8130U CPU with @ 2.21 GHz processor unit, installed random access memory (RAM), and SD drive of 256GB was used for the current docking studies. The Apo form of the protein was created in the PDB file using PDB Swiss Viewer, and the ligand was separated as a separate PDB file from the original protein-ligand complex PDB file (Doganc et al., 2021; Swain, 2014). Using the Open Babel software, a library SDF file of 17 planned derivatives for each scaffold from 1 to 3 was prepared (O'Boyle et al., 2011). Total 51 ligands were designed by 3 scaffolds of carbamate derivatives. Using different wizards such as the Open Babel wizard and the Vina wizard in the PyRx virtual screening tool software, the reference ligand and protein were prepared for docking, the compound SDF library was converted into PDBQT, and the Apo form of the protein and ligand libraries were docked (Dain et al., 123 C.E.; Tannas, 1985). Using the OpenBabel GUI tool and the ACD/ChemSketch chemical structure drawing application in ACS style, ligands were designed, prepared, and sketched in 2D, SD, and other necessary formats. The BIOVIA Discovery Studio Visualizer 2020 was used for the visualisations (Studio 2020, 2020). Protein Data Bank was a source that was found online to download the crystallographic pdb file (Berman et al., 2000)(*Protein Science - 2017 - Williams - MolProbity More and Better Reference Data for Improved All-atom Structure Validation.Pdf*, n.d.).

ISSN: 0975-3583,0976-2833 VOL14, ISSUE 07, 2023

Binding site interactions of ligand with protein:

With the use of BIOVIA Discovery Studio Visualizer 2020, the binding site interaction between the monoacylglycerol lipase enzyme and ligand complex, a catalytic triad, and oxyanion hole residues were all made visible. For the purpose of identifying and validating the binding region in the downloaded PDB file of a protein-ligand complex of 5ZUN, the protein PDB file 5ZUN was used to determine the existence of catalytic triad residues and oxyanion hole residues in the protein-ligand interaction site. The catalytic triad residues Ser122, His269, and Asp239 are located in the MAGL binding site (Bononi et al., 2018b; Riccardi et al., 2017). Downloaded from https://www.rcsb.org (Protein data bank), protein PDB file 5ZUN was examined for the residues in the ligand binding site. In the initial ligand-protein interaction site, catalytic triad residues Ser122, His269, and Asp239 were seen. Similarly, oxyanion hole residues Gly50, Ala51, Met123, and Gly124 were seen (Berdan et al., 2016; Sherer & Snape, 2015) in the binding site for ligand-protein interactions.

Docking Procedure:

1.1 Preparation of Protein:

For this work, the Monoacylglycerol Lipase X-ray Crystallographic Structure with the Ligand (9JX) with PDB ID: 5ZUN was used. Protein data bank (PDB) resources were retrieved from https://www.rcsb.org/ (*Protein Science - 2017 - Williams - MolProbity More and Better Reference Data for Improved All-atom Structure Validation.Pdf*, n.d.) in the PDB file format for the 3D X-ray crystallographic structure of the protein and ligand, and the MOLPROBITY service was used to prepare the protein's APO form (V. B. Chen et al., 2012; Davis et al., 2007). The MAGL protein molecule's PDB file was uploaded as part of the protein preparation process in order to fatching the protein from the MOLPROBITY server (PDB ID: 5ZUN). We then added hydrogens to it and used the "Make Flipkin kinemages illustrating any Asn, Gln, or His flips" option to accomplish the tasks of flipping the residues, examining all the atom connections, and analysing the molecule's geometry. The final protein file is downloaded by selecting "download" after the software has completed its task. The Swiss PDB reader was used to create the Apo form of the protein, which was then ready for protein preparation and docking with reference ligands (9JX) and ligands of various designs.

1.2 Preparation of Ligand:

Using a Swiss PDB viewer, the original ligand 9JX was dissociated from the protein-ligand complex and saved as a distinct file. This file served as the docking reference ligand. Based on the development of previously designed compounds as MAGL inhibitors, the two different scaffolds were created in this study. The key characteristics that were seen as being similar in the previously developed compound were taken into consideration for the creation of the new scaffolds. A total of 36 distinct derivatives were created from these two scaffolds. The 17 compounds that were created for each scaffold and employed as ligands are shown in Table 1. Using the ACS style option and OpenBabel GUI software, all of the structures of the relevant derivatives were generated using the ACD/ChemSketch molecular structure drawing application. When preparing ligands in PDBQT format for docking, the PyRx virtual screening tool's wizard also uses Open Babel. All of the ligands are minimised during the preparation process, and the ligands are then converted to the PDBQT format and the SDF file of the ligand library is inserted. The resultant stabilised structures were applied to the PyRx virtual screening tool's Vina wizard for protein-ligand docking.

ISSN: 0975-3583,0976-2833 VOL14, ISSUE 07, 2023

1.3 Validation studies:

Validation investigations of the MAGL protein crystal structure with an inhibitor ligand (9JX) (PDB ID: 5ZUN) (4R) -1-(2'-chloro[1,1'-biphenyl]-3-yl) four-[4-(1,3-thiazole-2-carbonyl) piperazin-1-yl] pyrrolidin-2-one]] was completed by redocking the separated file of the ligand (9JX) from the original PDB file (co-crystallized structure of the ligand) and the Apo form made of the MAGL protein file from 5ZUN into the precise binding site coordinates. For future use, the properties of the grid's coordinates were recorded.

1.4 Docking of Prepared protein and Ligand:

The Vina wizard in the PyRx virtual screening tool was utilised to carry out the planned ligands docking processes. The Apo protein file was uploaded to the MOLPROBITY Server, and the prepared protein file was downloaded from the server. Subsequently, the downloaded file was used for the redocking validation and docking of newly designed carbamate derivative ligands from TH101 – TH317. The protein and ligand complex were subjected to the Swiss PDB viewer, and the Apo form of the protein and separated ligand file were generated from it. The Open Babel software was used to create the ligand library in SDF format using smiles of all the designed ligands. These ligands were then minimised in the Open Babel wizard in the PyRx screening tool and converted to the AutoDock PDBQT format, and docking procedures were carried out using the AutoDock Vina wizard in the PyRx virtual screening tool. The grid box's dimensions were 25x25x25 in the x, y, and z directions for the grid creation procedure. The binding site interactions between the ligand 9JX and protein from the original PDB file served as the source for the attribute value coordinates. There was a 0.375 difference between each grid point. The chosen grid attributes are X = -13.07, Y = 20.8 and Z = -9.6. The molecular docking of each ligand with the produced protein was done using the PyRx virtual screening tool's Auto Dock Vina wizard (Carolina et al., n.d.). Using BIOVIA Discovery Studio Visualizer 2020, all docking results for various structures were analysed (Studio 2020, 2020).

2. ADME Studies

In order to further investigate the likelihood that a produced molecule will be used as a significant therapeutic in the treatment of disease, it is important to conduct Adsorption, Distribution, Metabolism, and Excretion (ADME) studies on the molecules. Various criteria, such as lipophilicity (iLOGP, XLOGP3, WLOGP, MLOGP, and SILICOS-IT), solubility in water [Log S (ESOL), Log S (Ali), and Log S (SILICOS-IT)] were predicted using the SWISSADME web-based application (http://www.swissadme.ch/), which was used to locate ADME research. drug-kinetic characteristics [(GI absorption, BBB permeation, P-gp substrate CYP2D6, CYP3A4 CYP1A2, CYP2C19, CYP2C9, inhibitor, Log Kp), Medicinal Chemistry (PAINS, Brenk, Leadlikeness, Synthetic accessibility), Druglikeness (Bioavailability Score Lipinski, Muegge, Ghose, Veber, Egan)] were also determined by using this SWISSADME web-based application (Pires et al., 2015).

The Swiss Institute of Bioinformatics' Molecular Modeling Group created and maintains the web server known as SWISSADME (SIB). Results were acquired by submitting SMILES of various structures and clicking RUN after doing so.

3. Toxicity Studies:

The pkCSM web server database's online ADMET prediction tool, which enables access to the analysis of molecules by drawing or by uploading in SMILES format, was used for toxicology

ISSN: 0975-3583,0976-2833 VOL14, ISSUE 07, 2023

investigations (Afzal et al., 2014). Data on toxicity includes AMES toxicity (Used to determine the carcinogenic effect of chemical), Max. tolerated dose (human), hERG I inhibitor, hERG II inhibitor (Used to determine cardiotoxicity), Oral Rat Chronic Toxicity (LOAEL), Oral Rat Acute Toxicity (LD50), Skin Sensitization, Hepatotoxicity, T. Pyriformis toxicity, and Minnow toxicity studies.

Results and Discussion

Docking Work

1. Target Binding Site Identification

JZL184 and Ly218324012, two previously synthesized monoacylglycerol lipase inhibitors, were reported to act through

Table 3. Molecular interactions of top three ligands from series 01, 02,03 and reference ligand.

S. No.	Ligand code	No. of conventional Hydrogen bonds	H-bond forming residues	H-bond distance (Å)	Hydrophobic residues
1	Ligand 9JX	3	ALA51, ARG57, MET123	2.09131, 2.14263, 2.19327	LEU241, TYR194, VAL191, VAL270, LYS273, ALA51, ILE179, LEU205
2	TH108	3	ALA51, MET123, UNK1	2.35572, 2.75475, 2.76253	ALA51, MET123, LEU241, VAL270, ALA151, VAL191, VAL270, LYS273
3	TH109	3	ALA51, MET123, UNK1	2.49203, 2.73384 2.86033	ALA51, MET123, LEU241, VAL270, ALA151, VAL270, LYS273
4	TH206	2	ALA51, MET123	2.19012, 2.34124	ALA51, MET123, GLY50, SER122, LEU241, VAL270:HG21, VAL191, VAL270, LYS273
5	TH208	3	ALA51, MET123, UNK1	2.41684, 2.76302 2.87057	ALA51, MET123, LEU241, VAL270, ALA151, VAL191, VAL270, LYS273, TYR194
6	TH306	3	ALA51, MET123, UNK1	2.21757, 2.34093 2.76974	ALA51, MET123, GLY50, SER122,

ISSN: 0975-3583,0976-2833 VOL14, ISSUE 07, 2023

					LEU241, VAL270, TYR194
7	TH308	3	ALA51, MET123, UNK1	2.48785, 2.81958 2.74682	ALA51, MET123, LEU241, VAL270, ALA151, TYR194

the catalytic triad amino acid residues Ser122, Asp239, and His269 and establish a covalent link with serine residue (Afzal et al., 2016). Ser122, Asp239, and His269 were found in the binding region of 9JX, which is shown in Fig. 1. The MAGL protein-ligand complex 5ZUN PDB file shows that interaction site of the ligand is the catalytic triad. Similar to this, the docking area of 9JX also exhibits Gly50, Ala51, Met123, and Gly124, confirming the existence of the oxyanion hole, which aids in stabilising the anionic transition state (Berdan et al., 2016). In order to cover the entire binding region, the same binding region was used with an increased grid size of 25 for XYZ dimensions for attributes X = -13.07, Y = 20.87, and Z = -9.62. The presence of these residues in the binding region of 9JX confirms the existence of a binding domain of the MAGL enzyme.

2. Validation studies:

By redocking the ligand (9JX) with a regenerated Apo form of the enzyme MAGL PDB file of 5ZUN, the vina wizard in the PyRx programme was used to validate the downloaded MAGL protein with ligand (PDB ID: 5ZUN). The ideal protein-ligand complex location was discovered to be superimposable with the ligand's optimum docking pose. According to the validation investigations, the binding energy for 9JX

Table 4. Swiss ADME studies data of top 2 ligands of series 01, series 02 and series 03.

Molecule	**TH108**	**TH109**	**TH206**	**TH208**	**TH306**	**TH308**
MR	125.68	130.48	112.54	122.15	110.33	119.95
TPSA	73.91	73.91	61.46	61.46	74.35	74.35
iLOGP	4.27	4.61	3.54	3.89	2.97	3.75
SILICOS-IT	5.11	5.51	3.22	4	2.65	3.43
Log S (ESOL), Class	-5.12	-5.47	-3.83	-4.45	-3.48	-4.11
Log S (Ali), Class	-5.86	-6.42	-3.66	-4.67	-3.35	-4.36
SILICOS-IT, Class	Poorly soluble	Poorly soluble	Poorly soluble	Poorly soluble	Moderately soluble	Poorly soluble
GI absorption	High	High	High	High	High	High
BBB permeant	Yes	Yes	Yes	Yes	No	Yes
Log Kp(skinperm.)	-5.55	-5.25	-6.59	-6.07	-7	-6.48
Lipinski	0	0	0	0	0	0
Ghosh	0	1	0	0	0	0
Veber	0	0	0	0	0	0
Egan	0	0	0	0	0	0

ISSN: 0975-3583,0976-2833 VOL14, ISSUE 07, 2023

Muegge	0	1	0	0	0	0
Bioavail. Score	0.55	0.55	0.55	0.55	0.55	0.55
PAINS	0	0	0	0	0	0
Brenk	0	0	0	0	0	0
Leadlikeness	3	3	1	3	1	2

was -13.4 kcal/mol. In Fig. 3, the redocking position is shown.

3. Docking Results:

In the form of binding energies with negative values, the results of the docking score of the ligands from TH101 to TH317 with apo form of 5ZUN MAGL protein are available in Table 1. Table 2. lists the best 3 docking results for 3 derivative ligands for each designed scaffold. 17 derivative ligands from each scaffold designed from 3 scaffold, total 51 ligands were subjected to the docking process with apo form of 5ZUN. Ligands TH113, TH115 from series 1, TH205, TH213, TH206 from series 2, TH305, TH313 and TH304 from series 3 displayed the best top nine docking scores. Table 3. lists the interactions with residues and hydrogen bonds for the top 9 ligands from the series 01, series 02 and series 03 based on docking scores. The change in the R substitution with electronegative atoms like NO2, F, Cl, Br, does not affected the docking score much, but the substitution with Cl, Br and F was observed no change in the docking score. Further the increase in chain length in alkyl substitution as R in all the 3 scaffolds, improvement in docking score is also observed. Replacement of hydrogen with alkyl chain in NH_2, as well as the increase the chain length with carbon does not causes any big change in the docking score. Similarly, the replacement of hydrogen with alkyl chain in OH as R substitution, also does not cause major changes in the docking score, however the propyl oxy is favourable for improvement in docking score. Whereas the R

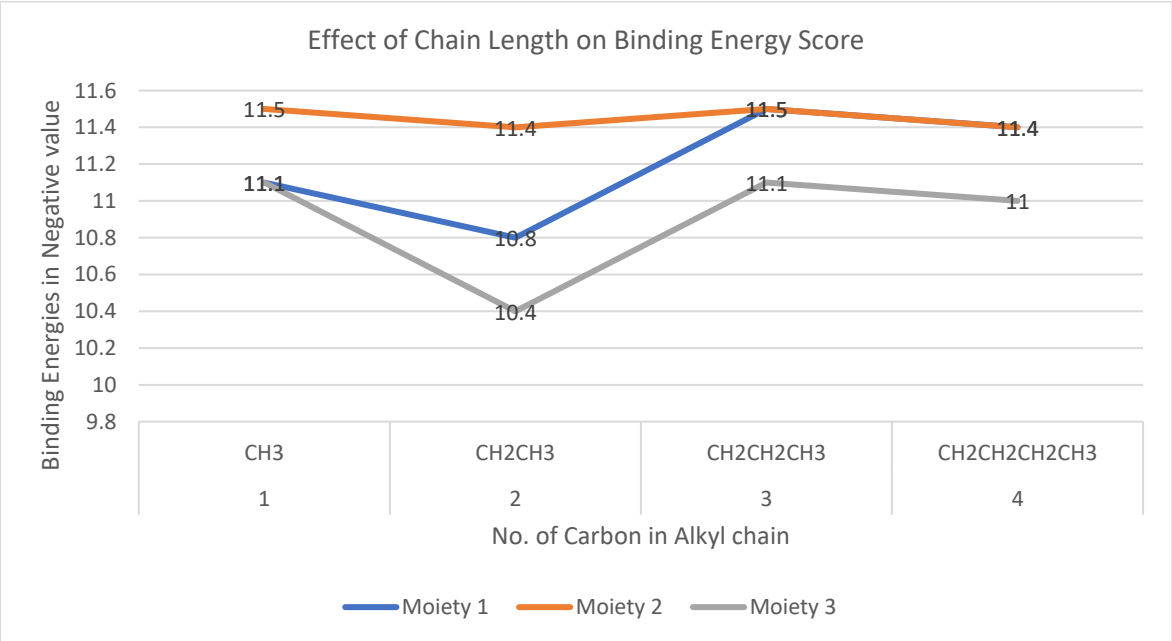

Fig. 9. Effect of Chain length on binding scores of ligands TH106, TH107, TH108, TH109, TH206, TH207, TH208, TH209, TH306, TH307, TH308, TH309 of series 01, 02 and 03.

ISSN: 0975-3583,0976-2833 VOL14, ISSUE 07, 2023

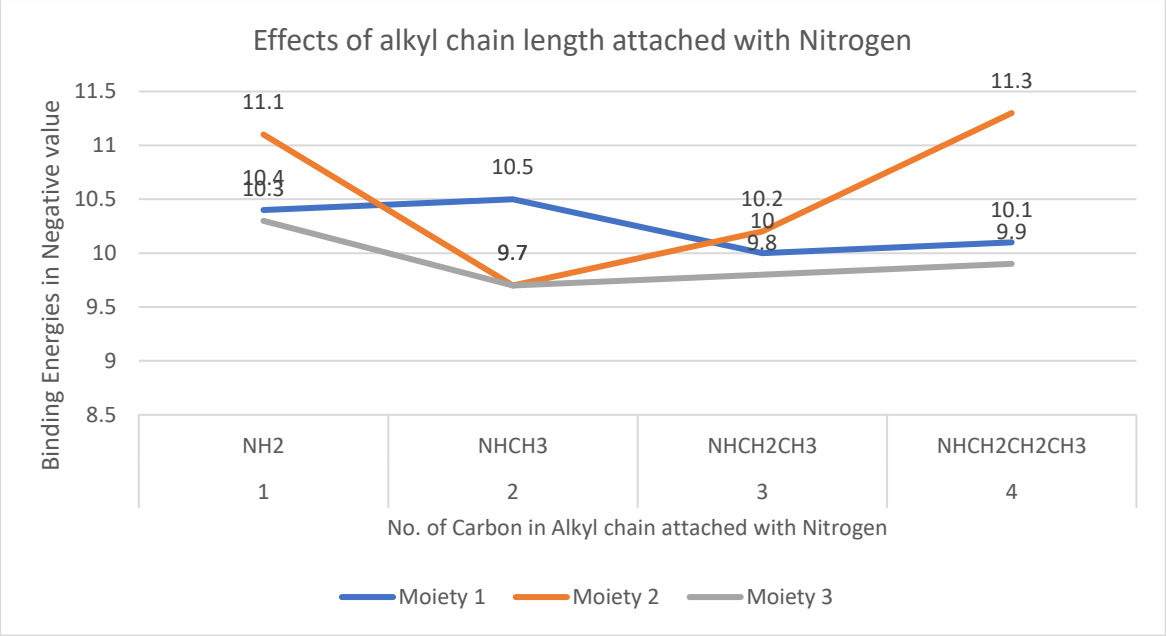

Fig. 10. Effect of Chain length attached with nitrogen on binding scores of ligands TH110, TH111, TH112, TH113, TH210, TH211, TH212, TH213, TH310, TH311, TH312, TH313 of series 01, 02 and 03.

substitution with alkyl chain is favourable for improvement in the docking score but improvement observed till increase in 3 carbons in alkyl chain. Replacement of the S with N at position 1 in thienopyridine ring favours for the improvement in the

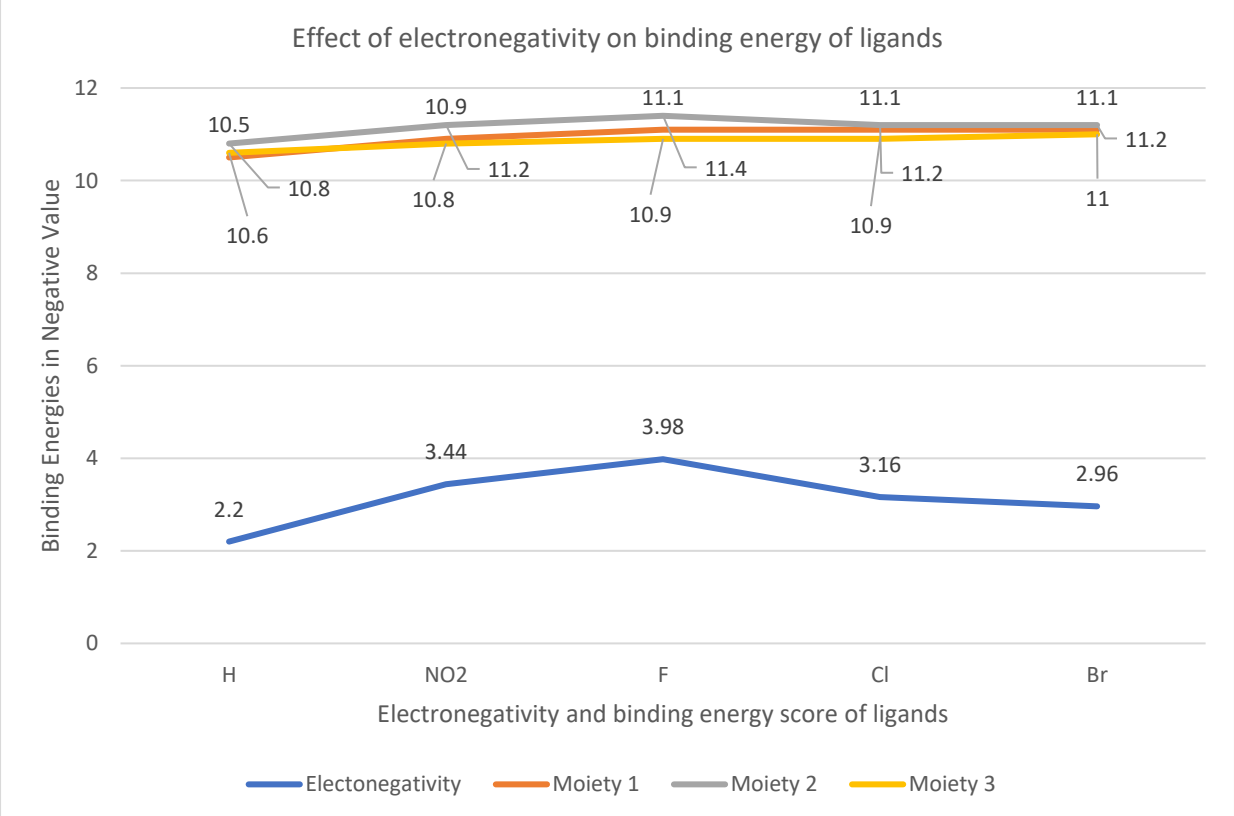

Fig. 11. Effect of electronegativity on binding scores of ligands TH101, TH102, TH103, TH104, TH105, TH201, TH202, TH203, TH204, TH205, TH301, TH302, TH303, TH304, TH305 of series 01, 02 and 03.

ISSN: 0975-3583,0976-2833 VOL14, ISSUE 07, 2023

Table 5. Predicted toxicity studies data of top 2 ligands of series 01, 02 and 03 by using pkCSM online tool.

Molecule	TH108	TH109	TH206	TH208	TH306	TH308
AMES toxicity	No	No	No	No	Yes	No
Max. tolerated dose (human)	-0.645	-0.561	-0.364	-0.465	0.781	0.704
hERG I inhibitor	No	No	No	No	No	No
hERG II inhibitor	Yes	Yes	Yes	Yes	Yes	Yes
Oral Rat Acute Toxicity (LD50)	2.843	2.844	2.911	3.006	2.438	2.47
Oral Rat Chronic Toxicity (LOAEL)	1.039	1.17	1.694	1.618	2.53	2.453
Hepatotoxicity	Yes	Yes	Yes	Yes	Yes	Yes
Skin Sensitisation	No	No	No	No	No	No
T. Pyriformis toxicity	0.589	0.567	0.324	0.343	0.285	0.285
Minnow toxicity	-0.278	-0.592	0.826	0.272	0.955	0.401

docking scores for all the designed derivatives compare to 01 series. Whereas the replacement of carbon with N in both 1 and 3 position in thienopyridine ring causes the decline in the docking score for all the derivatives of 03 series compare to 02 and 01 series. The docking poses images are depicted as from figure 2- 8. Fig. 9 – 11 shows the effects of changes in alkyl chain, changes in the length of alkyl chain with nitrogen, effects of electronegativity on docking scores.

Swiss ADME and toxicity Studies:

For additional analysis, such as ADME prediction were performed for the top two ligands from series 01, 02, and 03 TH108, TH109, TH206, TH208, TH306 and TH308 were subjected to the Swiss ADME studies and the data is represented in Table 5. Figures 2 – 5 show the 2D and 3D interaction photos for these top 2compounds of both the series. Whereas Table 5. Shows the predicted toxicity profile for top 2 best score compounds for the series 01, 02 and 03 by using pkCSM online tool.

Conclusion

In this study, 3 scaffolds and 51 derivatives of these scaffolds were designed. These 51 ligands were also the subject of studies on molecular docking. The top two molecules from the series 01, 02, and 03 were chosen for the Swiss ADME studies based on the best docking scores. All six of the top compounds displayed improved GI absorption, zero violations of the drug likeness requirements, and high synthetic accessibility scores. All of the compounds from series 01, 02, and 03 that received the two highest scores had their toxicity profiles and safety profiles for AMES toxicities, HERGI inhibition, and skin sensitization evaluated as well.

Acknowledgments: None.

Conflict of interest: None.

ISSN: 0975-3583,0976-2833 VOL14, ISSUE 07, 2023

Financial support: None.

Ethics statement: None

Reference:

1. Afzal, O., Akhtar, M. S., Kumar, S., Ali, M. R., Jaggi, M., & Bawa, S. (2016). Hit to lead optimization of a series of N-[4-(1,3-benzothiazol-2-yl)phenyl]acetamides as monoacylglycerol lipase inhibitors with potential anticancer activity. *European Journal of Medicinal Chemistry*. https://doi.org/10.1016/j.ejmech.2016.05.038
2. Afzal, O., Kumar, S., Kumar, R., Firoz, A., Jaggi, M., & Bawa, S. (2014). Docking based virtual screening and molecular dynamics study to identify potential monoacylglycerol lipase inhibitors. *Bioorganic and Medicinal Chemistry Letters*, *24*(16), 3986–3996. https://doi.org/10.1016/j.bmcl.2014.06.029
3. Ahamed, M., Attili, B., van Veghel, D., Ooms, M., Berben, P., Celen, S., Koole, M., Declercq, L., Savinainen, J. R., Laitinen, J. T., Verbruggen, A., & Bormans, G. (2017a). Synthesis and preclinical evaluation of [11C]MA-PB-1 for in vivo imaging of brain monoacylglycerol lipase (MAGL). *European Journal of Medicinal Chemistry*, *136*, 104–113. https://doi.org/10.1016/j.ejmech.2017.04.066
4. Ahamed, M., Attili, B., van Veghel, D., Ooms, M., Berben, P., Celen, S., Koole, M., Declercq, L., Savinainen, J. R., Laitinen, J. T., Verbruggen, A., & Bormans, G. (2017b). Synthesis and preclinical evaluation of [11C]MA-PB-1 for in vivo imaging of brain monoacylglycerol lipase (MAGL). *European Journal of Medicinal Chemistry*. https://doi.org/10.1016/j.ejmech.2017.04.066
5. Aida, J., Fushimi, M., Kusumoto, T., Sugiyama, H., Arimura, N., Ikeda, S., Sasaki, M., Sogabe, S., Aoyama, K., & Koike, T. (2018). Design, Synthesis, and Evaluation of Piperazinyl Pyrrolidin-2-ones as a Novel Series of Reversible Monoacylglycerol Lipase Inhibitors. *Journal of Medicinal Chemistry*. https://doi.org/10.1021/acs.jmedchem.8b00824
6. Berdan, C. A., Erion, K. A., Burritt, N. E., Corkey, B. E., & Deeney, J. T. (2016). Inhibition of monoacylglycerol lipase activity decreases glucose-stimulated insulin secretion in INS-1 (832/13) cells and rat islets. *PLoS ONE*, *11*(2), e0149008. https://doi.org/10.1371/journal.pone.0149008
7. Berman, H. M., Westbrook, J., Feng, Z., Gilliland, G., Bhat, T. N., Weissig, H., Shindyalov, I. N., & Bourne, P. E. (2000). The Protein Data Bank. *Nucleic Acids Research*, *28*(1), 235–242. https://doi.org/10.1093/NAR/28.1.235
8. Bononi, G., Granchi, C., Lapillo, M., Giannotti, M., Nieri, D., Fortunato, S., Boustani, M. El, Caligiuri, I., Poli, G., Carlson, K. E., Kim, S. H., Macchia, M., Martinelli, A., Rizzolio, F., Chicca, A., Katzenellenbogen, J. A., Minutolo, F., & Tuccinardi, T. (2018a). Discovery of long-chain salicylketoxime derivatives as monoacylglycerol lipase (MAGL) inhibitors. *European Journal of Medicinal Chemistry*, *157*, 817–836. https://doi.org/10.1016/j.ejmech.2018.08.038
9. Bononi, G., Granchi, C., Lapillo, M., Giannotti, M., Nieri, D., Fortunato, S., Boustani, M. El, Caligiuri, I., Poli, G., Carlson, K. E., Kim, S. H., Macchia, M., Martinelli, A., Rizzolio, F., Chicca, A., Katzenellenbogen, J. A., Minutolo, F., & Tuccinardi, T.

ISSN: 0975-3583,0976-2833 VOL14, ISSUE 07, 2023

(2018b). Discovery of long-chain salicylketoxime derivatives as monoacylglycerol lipase (MAGL) inhibitors. *European Journal of Medicinal Chemistry*. https://doi.org/10.1016/j.ejmech.2018.08.038

10. Butler, C. R., Beck, E. M., Harris, A., Huang, Z., McAllister, L. A., Am Ende, C. W., Fennell, K., Foley, T. L., Fonseca, K., Hawrylik, S. J., Johnson, D. S., Knafels, J. D., Mente, S., Noell, G. S., Pandit, J., Phillips, T. B., Piro, J. R., Rogers, B. N., Samad, T. A., … Brodney, M. A. (2017). Azetidine and Piperidine Carbamates as Efficient, Covalent Inhibitors of Monoacylglycerol Lipase. *Journal of Medicinal Chemistry*. https://doi.org/10.1021/acs.jmedchem.7b01531
11. Carolina, A., De Sousa, C., Combrinck, J. M., Maepa, K., & Egan, T. J. (n.d.). *Virtual screening as a tool to discover new β-haematin inhibitors with activity against malaria parasites*. https://doi.org/10.1038/s41598-020-60221-0
12. Castelli, R., Scalvini, L., Vacondio, F., Lodola, A., Anselmi, M., Vezzosi, S., Carmi, C., Bassi, M., Ferlenghi, F., Rivara, S., Møller, I. R., Rand, K. D., Daglian, J., Wei, D., Dotsey, E. Y., Ahmed, F., Jung, K. M., Stella, N., Singh, S., … Piomelli, D. (2020). Benzisothiazolinone Derivatives as Potent Allosteric Monoacylglycerol Lipase Inhibitors That Functionally Mimic Sulfenylation of Regulatory Cysteines. *Journal of Medicinal Chemistry*. https://doi.org/10.1021/acs.jmedchem.9b01679
13. Chen, V. B., Arendall, W. B., Headd, J. J., Keedy, D. A., Immormino, R. M., Kapral, G. J., Murray, L. W., Richardson, J. S., & Richardson, D. C. (2012). *MolProbity : all-atom structure validation for macromolecular crystallography* . 694–701. https://doi.org/10.1107/97809553602060000884
14. Chen, Z., Mori, W., Deng, X., Cheng, R., Ogasawara, D., Zhang, G., Schafroth, M. A., Dahl, K., Fu, H., Hatori, A., Shao, T., Zhang, Y., Yamasaki, T., Zhang, X., Rong, J., Yu, Q., Hu, K., Fujinaga, M., Xie, L., … Liang, S. H. (2019). Design, Synthesis, and Evaluation of Reversible and Irreversible Monoacylglycerol Lipase Positron Emission Tomography (PET) Tracers Using a “tail Switching” Strategy on a Piperazinyl Azetidine Skeleton. *Journal of Medicinal Chemistry*. https://doi.org/10.1021/acs.jmedchem.8b01778
15. Chen, Z., Mori, W., Fu, H., Schafroth, M. A., Hatori, A., Shao, T., Zhang, G., Van, R. S., Zhang, Y., Hu, K., Fujinaga, M., Wang, L., Belov, V., Ogasawara, D., Giffenig, P., Deng, X., Rong, J., Yu, Q., Zhang, X., … Liang, S. H. (2019). Design, Synthesis, and Evaluation of 18F-Labeled Monoacylglycerol Lipase Inhibitors as Novel Positron Emission Tomography Probes. *Journal of Medicinal Chemistry*. https://doi.org/10.1021/acs.jmedchem.9b00936
16. Cisar, J. S., Weber, O. D., Clapper, J. R., Blankman, J. L., Henry, C. L., Simon, G. M., Alexander, J. P., Jones, T. K., Ezekowitz, R. A. B., O’Neill, G. P., & Grice, C. A. (2018). Identification of ABX-1431, a Selective Inhibitor of Monoacylglycerol Lipase and Clinical Candidate for Treatment of Neurological Disorders. *Journal of Medicinal Chemistry*. https://doi.org/10.1021/acs.jmedchem.8b00951
17. Dain, F. A., Opo, M., Rahman, M. M., Ahammad, F., Ahmed, I., Bhuiyan, A., & Asiri, A. M. (123 C.E.). Structure based pharmacophore modeling, virtual screening, molecular docking and ADMET approaches for identification of natural anti-cancer agents targeting XIAP protein. *Scientific Reports |*, *11*, 4049.

ISSN: 0975-3583,0976-2833 VOL14, ISSUE 07, 2023

https://doi.org/10.1038/s41598-021-83626-x

18. Dato, F. M., Neudörfl, J. M., Gütschow, M., Goldfuss, B., & Pietsch, M. (2020). ω-Quinazolinonylalkyl aryl ureas as reversible inhibitors of monoacylglycerol lipase. *Bioorganic Chemistry*. https://doi.org/10.1016/j.bioorg.2019.103352
19. Davis, I. W., Leaver-Fay, A., Chen, V. B., Block, J. N., Kapral, G. J., Wang, X., Murray, L. W., Arendall, W. B., Snoeyink, J., Richardson, J. S., & Richardson, D. C. (2007). MolProbity: all-atom contacts and structure validation for proteins and nucleic acids. *Nucleic Acids Research*, *35*(suppl_2), W375–W383. https://doi.org/10.1093/NAR/GKM216
20. Doganc, F., Celik, I., Eren, G., Kaiser, M., Brun, R., & Goker, H. (2021). Synthesis, in vitro antiprotozoal activity, molecular docking and molecular dynamics studies of some new monocationic guanidinobenzimidazoles. *European Journal of Medicinal Chemistry*, *221*, 113545. https://doi.org/10.1016/j.ejmech.2021.113545
21. Granchi, C., Lapillo, M., Glasmacher, S., Bononi, G., Licari, C., Poli, G., El Boustani, M., Caligiuri, I., Rizzolio, F., Gertsch, J., Macchia, M., Minutolo, F., Tuccinardi, T., & Chicca, A. (2019). Optimization of a Benzoylpiperidine Class Identifies a Highly Potent and Selective Reversible Monoacylglycerol Lipase (MAGL) Inhibitor. *Journal of Medicinal Chemistry*. https://doi.org/10.1021/acs.jmedchem.8b01483
22. Granchi, C., Rizzolio, F., Caligiuri, I., Macchia, M., Martinelli, A., Minutolo, F., & Tuccinardi, T. (2018). Rational development of MAGL inhibitors. *Methods in Molecular Biology*, *1824*(c), 335–346. https://doi.org/10.1007/978-1-4939-8630-9_20
23. Hattori, Y., Aoyama, K., Maeda, J., Arimura, N., Takahashi, Y., Sasaki, M., Fujinaga, M., Seki, C., Nagai, Y., Kawamura, K., Yamasaki, T., Zhang, M. R., Higuchi, M., & Koike, T. (2019). Design, Synthesis, and Evaluation of (4 R)-1-{3-[2-(18F)Fluoro-4-methylpyridin-3-yl]phenyl}-4-[4-(1,3-thiazol-2-ylcarbonyl)piperazin-1-yl]pyrrolidin-2-one ([18F] T-401) as a Novel Positron-Emission Tomography Imaging Agent for Monoacylglycerol Lipase. *Journal of Medicinal Chemistry*. https://doi.org/10.1021/acs.jmedchem.8b01576
24. Jiang, M., & Van Der Stelt, M. (2018). Activity-Based Protein Profiling Delivers Selective Drug Candidate ABX-1431, a Monoacylglycerol Lipase Inhibitor, to Control Lipid Metabolism in Neurological Disorders. In *Journal of Medicinal Chemistry*. https://doi.org/10.1021/acs.jmedchem.8b01405
25. Jung, K. M., & Piomelli, D. (2016). Assay of monoacylglycerol lipase activity. In *Methods in Molecular Biology* (Vol. 1412, pp. 157–168). Humana Press Inc. https://doi.org/10.1007/978-1-4939-3539-0_17
26. Karageorgos, I., Silin, V. I., Zvonok, N., Marino, J., Janero, D. R., & Makriyannis, A. (2017). The role of human monoacylglycerol lipase (hMAGL) binding pocket in breakup of unsaturated phospholipid membranes. *Analytical Biochemistry*, *536*, 90–95. https://doi.org/10.1016/j.ab.2017.08.009
27. Kind, L., & Kursula, P. (2019). Structural properties and role of the endocannabinoid lipases ABHD6 and ABHD12 in lipid signalling and disease. In *Amino Acids*. https://doi.org/10.1007/s00726-018-2682-8
28. King, A. R., Dotsey, E. Y., Lodola, A., Jung, K. M., Ghomian, A., Qiu, Y., Fu, J., Mor, M., & Piomelli, D. (2009). Discovery of Potent and Reversible Monoacylglycerol

ISSN: 0975-3583,0976-2833 VOL14, ISSUE 07, 2023

Lipase Inhibitors. *Chemistry and Biology*. https://doi.org/10.1016/j.chembiol.2009.09.012

29. Kohnz, R. A., & Nomura, D. K. (2014). Chemical approaches to therapeutically target the metabolism and signaling of the endocannabinoid 2-AG and eicosanoids. In *Chemical Society Reviews* (Vol. 43, Issue 19, pp. 6859–6869). Royal Society of Chemistry. https://doi.org/10.1039/c4cs00047a
30. Kumar Verma, A., Farswan Singh, M., & Awasthi, A. (2021). Role of p38 MAP Kinase Inhibitor (SB239063) and Vitamin B12 against Neuroinflammation. *International Journal of Pharmaceutical Investigation*, *11*(1), 94–98. https://doi.org/10.5530/ijpi.2021.1.17
31. Liu, X., Chen, Y., Vickstrom, C. R., Li, Y., Viader, A., Cravatt, B. F., & Liu, Q. S. (2016). Coordinated regulation of endocannabinoid-mediated retrograde synaptic suppression in the cerebellum by neuronal and astrocytic monoacylglycerol lipase. *Scientific Reports*, *6*(1), 1–10. https://doi.org/10.1038/srep35829
32. Ma, M., Bai, J., Ling, Y., Chang, W., Xie, G., Li, R., Wang, G., & Tao, K. (2016). Monoacylglycerol lipase inhibitor JZL184 regulates apoptosis and migration of colorectal cancer cells. *Molecular Medicine Reports*, *13*(3), 2850–2856. https://doi.org/10.3892/mmr.2016.4829
33. Malamas, M. S., Farah, S. I., Lamani, M., Pelekoudas, D. N., Perry, N. T., Rajarshi, G., Miyabe, C. Y., Chandrashekhar, H., West, J., Pavlopoulos, S., & Makriyannis, A. (2020). Design and synthesis of cyanamides as potent and selective N-acylethanolamine acid amidase inhibitors. *Bioorganic and Medicinal Chemistry*, *28*(1), 115195. https://doi.org/10.1016/j.bmc.2019.115195
34. McAllister, L. A., Butler, C. R., Mente, S., O'Neil, S. V., Fonseca, K. R., Piro, J. R., Cianfrogna, J. A., Foley, T. L., Gilbert, A. M., Harris, A. R., Helal, C. J., Johnson, D. S., Montgomery, J. I., Nason, D. M., Noell, S., Pandit, J., Rogers, B. N., Samad, T. A., Shaffer, C. L., … Brodney, M. A. (2018). Discovery of Trifluoromethyl Glycol Carbamates as Potent and Selective Covalent Monoacylglycerol Lipase (MAGL) Inhibitors for Treatment of Neuroinflammation. *Journal of Medicinal Chemistry*. https://doi.org/10.1021/acs.jmedchem.8b00070
35. Miceli, M., Casati, S., Ottria, R., Di Leo, S., Eberini, I., Palazzolo, L., Parravicini, C., & Ciuffreda, P. (2019). Set-up and validation of a high throughput screening method for human monoacylglycerol lipase (MAGL) based on a new red fluorescent probe. *Molecules*. https://doi.org/10.3390/molecules24122241
36. Mori, W., Hatori, A., Zhang, Y., Kurihara, Y., Yamasaki, T., Xie, L., Kumata, K., Hu, K., Fujinaga, M., & Zhang, M. R. (2019). Radiosynthesis and evaluation of a novel monoacylglycerol lipase radiotracer: 1,1,1,3,3,3-hexafluoropropan-2-yl-3-(1-benzyl-1H-pyrazol-3-yl)azetidine-1-[11C]carboxylate. *Bioorganic and Medicinal Chemistry*, *27*(16), 3568–3573. https://doi.org/10.1016/j.bmc.2019.06.037
37. O'Boyle, N. M., Banck, M., James, C. A., Morley, C., Vandermeersch, T., & Hutchison, G. R. (2011). Open Babel. *Journal of Cheminformatics*, *3*(33), 1–14. https://jcheminf.biomedcentral.com/track/pdf/10.1186/1758-2946-3-33
38. Patel, J. Z., Nevalainen, T. J., Savinainen, J. R., Adams, Y., Laitinen, T., Runyon, R. S., Vaara, M., Ahenkorah, S., Kaczor, A. A., Navia-Paldanius, D., Gynther, M.,

ISSN: 0975-3583,0976-2833 VOL14, ISSUE 07, 2023

Aaltonen, N., Joharapurkar, A. A., Jain, M. R., Haka, A. S., Maxfield, F. R., Laitinen, J. T., & Parkkari, T. (2015). Optimization of 1,2,5-Thiadiazole Carbamates as Potent and Selective ABHD6 Inhibitors. *ChemMedChem*, *10*(2), 253–265. https://doi.org/10.1002/cmdc.201402453

39. Pires, D. E. V., Blundell, T. L., & Ascher, D. B. (2015). pkCSM: Predicting small-molecule pharmacokinetic and toxicity properties using graph-based signatures. *Journal of Medicinal Chemistry*, *58*(9), 4066–4072. https://doi.org/10.1021/acs.jmedchem.5b00104
40. *Protein Science - 2017 - Williams - MolProbity More and better reference data for improved all-atom structure validation.pdf*. (n.d.).
41. Riccardi, L., Arencibia, J. M., Bono, L., Armirotti, A., Girotto, S., & De Vivo, M. (2017). Lid domain plasticity and lipid flexibility modulate enzyme specificity in human monoacylglycerol lipase. *Biochimica et Biophysica Acta - Molecular and Cell Biology of Lipids*, *1862*(5), 441–451. https://doi.org/10.1016/j.bbalip.2017.01.002
42. Scalvini, L., Piomelli, D., & Mor, M. (2016). Monoglyceride lipase: Structure and inhibitors. *Chemistry and Physics of Lipids*, *197*, 13–24. https://doi.org/10.1016/j.chemphyslip.2015.07.011
43. Scalvini, L., Vacondio, F., Bassi, M., Pala, D., Lodola, A., Rivara, S., Jung, K. M., Piomelli, D., & Mor, M. (2016a). Free-energy studies reveal a possible mechanism for oxidation-dependent inhibition of MGL. *Scientific Reports*, *6*(April), 1–12. https://doi.org/10.1038/srep31046
44. Scalvini, L., Vacondio, F., Bassi, M., Pala, D., Lodola, A., Rivara, S., Jung, K. M., Piomelli, D., & Mor, M. (2016b). Free-energy studies reveal a possible mechanism for oxidation-dependent inhibition of MGL. *Scientific Reports*, *6*(1), 1–12. https://doi.org/10.1038/srep31046
45. Sherer, C., & Snape, T. J. (2015). Heterocyclic scaffolds as promising anticancer agents against tumours of the central nervous system: Exploring the scope of indole and carbazole derivatives. In *European Journal of Medicinal Chemistry* (Vol. 97, Issue 1, pp. 552–560). Elsevier Masson s.r.l. https://doi.org/10.1016/j.ejmech.2014.11.007
46. Studio 2020, B. D. (2020). Dassault Systems: San Diego. *CA, USA*.
47. Swain, C. (2014). *Open Babel Documentation*.
48. Tannas, L. E. (1985). System Requirements. *Flat-Panel Displays and CRTs*, 31–53. https://doi.org/10.1007/978-94-011-7062-8_2
49. Verma, A. K., Singh, M. F., & Awasthi, A. (2021). Neuroprotective Effect of p38 MAPKs Inhibitor (SB239063) and Vitamin B12 against Lipopolysaccharide Induced Neuroinflammation. *International Journal of Pharmaceutical Investigation*, *11*(1), 99–103. https://doi.org/10.5530/ijpi.2021.1.18
50. Wang, L., Mori, W., Cheng, R., Yui, J., Hatori, A., Ma, L., Zhang, Y., Rotstein, B. H., Fujinaga, M., Shimoda, Y., Yamasaki, T., Xie, L., Nagai, Y., Minamimoto, T., Higuchi, M., Vasdev, N., Zhang, M. R., & Liang, S. H. (2016). Synthesis and preclinical evaluation of sulfonamidobased [11C-Carbonyl]-carbamates and ureas for imaging monoacylglycerol lipase. *Theranostics*, *6*(8), 1145–1159. https://doi.org/10.7150/thno.15257
51. Wise, L. E., Long, K. A., Abdullah, R. A., Long, J. Z., Cravatt, B. F., & Lichtman, A.

ISSN: 0975-3583,0976-2833 VOL14, ISSUE 07, 2023

H. (2012). Dual fatty acid amide hydrolase and monoacylglycerol lipase blockade produces THC-like morris water maze deficits in mice. *ACS Chemical Neuroscience*, *3*(5), 369–378. https://doi.org/10.1021/cn200130s

52. Zhang, J., Liu, Z., Lian, Z., Liao, R., Chen, Y., Qin, Y., Wang, J., Jiang, Q., Wang, X., & Gong, J. (2016). Monoacylglycerol Lipase: A Novel Potential Therapeutic Target and Prognostic Indicator for Hepatocellular Carcinoma. *Scientific Reports*. https://doi.org/10.1038/srep35784
53. Zhang, L., Butler, C. R., Maresca, K. P., Takano, A., Nag, S., Jia, Z., Arakawa, R., Piro, J. R., Samad, T., Smith, D. L., Nason, D. M., O'Neil, S., McAllister, L., Schildknegt, K., Trapa, P., McCarthy, T. J., Villalobos, A., & Halldin, C. (2019). Identification and Development of an Irreversible Monoacylglycerol Lipase (MAGL) Positron Emission Tomography (PET) Radioligand with High Specificity. *Journal of Medicinal Chemistry*. https://doi.org/10.1021/acs.jmedchem.9b00847